Receptor tyrosine kinase-like orphan receptor 2 (ROR2) and Indian hedgehog regulate digit outgrowth mediated by the phalanx-forming region

Florian Witte[a,b,c], Danny Chan[d], Aris N. Economides[e], Stefan Mundlos[a,b,f], and Sigmar Stricker[a,b,1]

[a]Development and Disease Group, Max Planck Institute for Molecular Genetics, 14195 Berlin, Germany; [b]Institute for Medical Genetics, Charité, University Medicine Berlin, 13353 Berlin, Germany; [c]Institut für Chemie/Biochemie, Freie Universität Berlin, 14195 Berlin, Germany; [d]Department of Biochemistry, The University of Hong Kong, Pokfulam, Hong Kong, China; [e]Regeneron Pharmaceuticals, Inc., Tarrytown, NY 10591; and [f]Berlin-Brandenburg Center for Regenerative Therapies, Charité, University Medicine Berlin, 13353 Berlin, Germany

Communicated by George D. Yancopoulos, Regeneron Pharmaceuticals, Inc., Tarrytown, NY, June 30, 2010 (received for review March 1, 2010)

Elongation of the digit rays resulting in the formation of a defined number of phalanges is a process poorly understood in mammals, whereas in the chicken distal mesenchymal bone morphogenetic protein (BMP) signaling in the so-called phalanx-forming region (PFR) or digit crescent (DC) seems to be involved. The human brachydactylies (BDs) are inheritable conditions characterized by variable degrees of digit shortening, thus providing an ideal model to analyze the development and elongation of phalanges. We used a mouse model for BDB1 (*Ror2*$^{W749X/W749X}$) lacking middle phalanges and show that a signaling center corresponding to the chick PFR exists in the mouse, which is diminished in BDB1 mice. This resulted in a strongly impaired elongation of the digit condensations due to reduced chondrogenic commitment of undifferentiated distal mesenchymal cells. We further show that a similar BMP-based mechanism accounts for digit shortening in a mouse model for the closely related condition BDA1 (*Ihh*$^{E95K/E95K}$), altogether indicating the functional significance of the PFR in mammals. Genetic interaction experiments as well as pathway analysis in BDB1 mice suggest that Indian hedgehog and WNT/β-catenin signaling, which we show is inhibited by receptor tyrosine kinase-like orphan receptor 2 (ROR2) in distal limb mesenchyme, are acting upstream of BMP signaling in the PFR.

bone morphogenetic protein signaling | brachydactyly | cartilage | limb development | Wnt signaling

The appendicular skeleton arises as a continuous cartilaginous condensation in the center of the limb bud that develops in a proximal to distal sequence. Distal outgrowth is under the control of fibroblast growth factor (FGF) signaling from the apical ectodermal ridge (AER), which accounts for proliferation in the subridge mesenchyme and prevents premature differentiation of mesenchymal cells, thus maintaining a progenitor pool. Cells leaving the range of AER-FGF signaling undergo differentiation into the mesenchymal cell lineages of the limb bud (1, 2).

Evidence from the chick indicates that bone morphogenetic protein (BMP)/pSMAD1/5/8 signaling in a population of cells in front of the growing condensation, referred to as the phalanx-forming region (PFR) or digit crescent (3, 4), is involved in the elongation of the digital rays. This work suggests that the PFR acts as a signaling center to drive distal elongation of the digit and thus determines the number of phalanges via commitment of distal mesenchymal cells to the cartilage condensation. However, evidence for such a mechanism in the mouse or human is missing.

If a PFR-like structure exists in mammals, its failure is expected to cause digit malformation phenotypes such as digit shortening and loss of phalanges. This phenotypic spectrum is typical for a family of human inheritable malformations, the brachydactylies (BDs), which are characterized by the absence or reduction of individual phalanges and/or metacarpals (5). Intriguingly, several mutations causing human BDs (BDA2, BDB2, and BDC) affect the BMP pathway (5), which suggests the involvement of a PFR-like structure in digit growth.

BD types A1 and B1 are of particular interest, because they show a generalized reduction defect in specific phalanges. BDA1 is characterized by shortening/absence of all middle phalanges. BDB1 is characterized by an amputation-like phenotype with shortening/absence of distal and often middle phalanges. Human BDA1 and BDB1 are caused by mutations in *Indian hedgehog* (*IHH*) or *receptor tyrosine kinase-like orphan receptor 2 (ROR2)*, respectively (5). IHH is a factor required for endochondral ossification. BDA1 mutations change the signaling capacity and range of IHH, thereby altering distal chondrogenesis (6). *ROR2* encodes a receptor tyrosine kinase, which is truncated by BDB1 mutations. The function of ROR2 is not fully understood, and there is evidence suggesting that ROR2 functions as a WNT (co)receptor (7). For example, it was shown that WNT5A via ROR2 can inhibit canonical WNT/β-catenin signaling (8).

Mouse models for BDA1 and BDB1 generated by targeted insertion of human mutations into the mouse *Ihh* and *Ror2* loci partially recapitulate these phenotypes. BDA1 mice with a p.E95K mutation in *Ihh* (6) show shortened middle phalanges, whereas BDB1 mice with a p.W749X mutation in *Ror2* (9) exhibit absent middle phalanges; thus the BDB1 and BDA1 mice present a graded digit reduction phenotype.

To address the mechanism controlling the outgrowth of the digital rays in mammals, we first analyzed the BDB1 mouse, demonstrating that a mesenchymal cell population corresponding to the chick PFR exists in the mouse, contributing to mammalian digit elongation. Consistent with the overlapping but milder phenotype of the BDA1 mice, a milder disruption of the PFR was observed, indicating that a graded decrease in BMP/pSMAD1/5/8 signaling in the PFR might account for different BD phenotypes. From further genetic studies, we propose a model in which IHH, ROR2, and WNT signaling regulate PFR activity.

Results

Brachydactyly in Ror2$^{W749X/W749X}$ Mutants Corresponds to Decreased BMP/pSMAD1/5/8 Signaling in the PFR. First, we used the *Ror2*$^{W749X/W749X}$ mice (BDB1 model) to test for the existence and function of a PFR in mammals. The avian PFR has been characterized by the expression of *BmpR1b*, *Sox9*, and a high activity of the BMP signal mediators phospho-SMAD1/5/8 (pSMAD1/5/8) (3, 4). Analysis of *BmpR1b* expression in *Ror2*$^{W749X/W749X}$ mice by whole-mount in situ hybridization (ISH) showed a reduced distal signal and an increased distance between the most distal *BmpR1b* expression and the ectoderm (Fig. 1*A*). Immunostaining for SOX9

Author contributions: F.W. and S.S. performed research; F.W. and S.S. analyzed data; D.C. and A.N.E. contributed new reagents/analytic tools; S.M. and S.S. designed research; and S.S. wrote the paper.

The authors declare no conflict of interest.

[1]To whom correspondence should be addressed. E-mail: strick_s@molgen.mpg.de.

This article contains supporting information online at www.pnas.org/lookup/suppl/doi:10.1073/pnas.1009314107/-/DCSupplemental.

DEVELOPMENTAL BIOLOGY

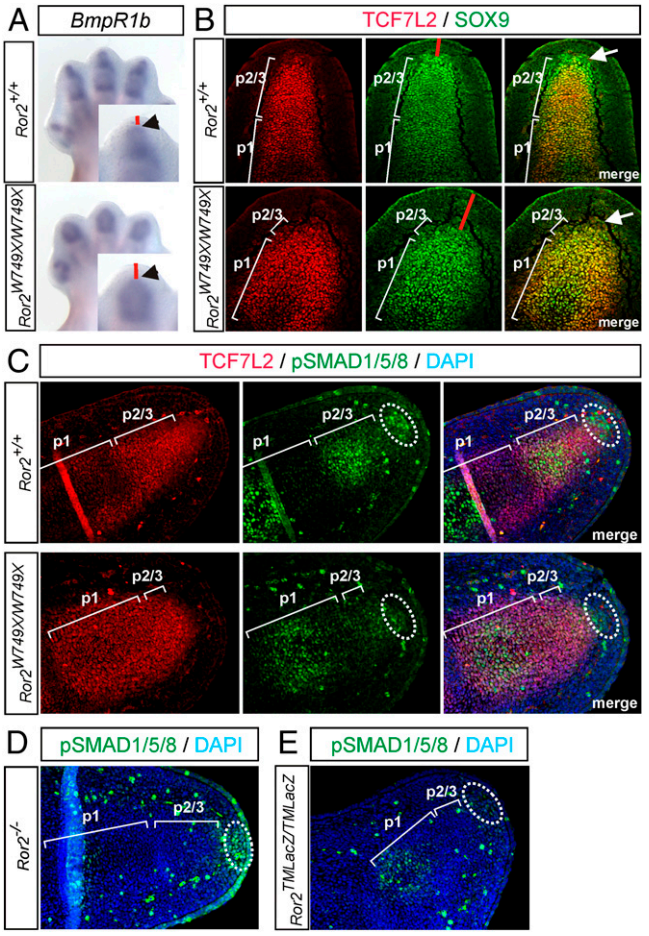

Fig. 1. Existence of the PFR in the mouse and its disruption in *Ror2*$^{W749X/W749X}$ mutants. (*A*) Whole-mount ISH showing missing expression of *BmpR1b* in distal-most mesenchyme (arrowheads) and expanded distance between *BmpR1b* expression and ectoderm (red bars) in the *Ror2*$^{W749X/W749X}$ mutant. (*B*) Immunostaining for TCF7L2 marking the cartilage condensation (red) and SOX9 (green) marking chondrogenic progenitors shows a domain of SOX9 expressing cells distal to definitive cartilage in the WT, which is absent in the *Ror2*$^{W749X/W749X}$ mutant (arrows). Note the increased distance between SOX9 expression and ectoderm (red bars) in the *Ror2*$^{W749X/W749X}$ mutant. (*C*) Immunostaining for phospho-SMAD1/5/8 (green) revealing the presence of a PFR in WT mouse embryos at E13.5 (dotted circle). This population of pSMAD1/5/8-positive cells is lacking in the *Ror2*$^{W749X/W749X}$ mutant. (*D*) Immunolabeling for pSMAD1/5/8 shows normal staining in the distal mesenchyme in *Ror2*$^{-/-}$ mutants, whereas in *Ror2*$^{TMLacZ/TMLacZ}$ mutants (*E*) pSMAD1/5/8 staining is diminished. p1, condensation of phalanx 1; p2/3, unseparated primordium of phalanges 2 and 3.

colabeled for TCF7L2, which stains the nascent condensation, revealed a population of cells expressing SOX9 distal to the cartilaginous condensation at embryonic day 13.5 (E13.5) in WT mice (Fig. 1*B*). In *Ror2*$^{W749X/W749X}$ mice, this population of SOX9 positive cells was absent, and the distance between the distal SOX9 expression region and the ectoderm was increased (Fig. 1*B*). Furthermore, immunostaining for pSMAD1/5/8 revealed a population of mesenchymal cells distal to the definitive cartilage that was strongly positive for active BMP signaling in WT mice (Fig. 1*C*), overlapping the population of Sox9-positive cells described above. These findings indicate that a region similar to the PFR described in the chick is also present in the mouse. In *Ror2*$^{W749X/W749X}$ mice, vastly decreased pSMAD1/5/8 staining in the distal mesenchymal population indicates a breakdown of BMP/SMAD signaling in the distal mesenchyme (Fig. 1*C*).

Ror2$^{-/-}$ mice do not show a reduction of the middle phalanx (p2), indicating that the *Ror2*^{W749X} allele has a gain-of-function effect, which was supported by crossing one *Ror2*^{W749X} allele on a Ror2-null background, yielding an intermediate phenotype (Fig. S1). Consistently, analysis of pSMAD1/5/8 in *Ror2*$^{-/-}$ mice showed a normal PFR staining similar to WT mice (Fig. 1*D*). To further test the involvement of the PFR in the brachydactyly phenotype, we analyzed *Ror2*$^{TMLacZ/TMLacZ}$ mice, which display a digit phenotype comparable to the *Ror2*$^{W749X/W749X}$ mice. As expected, *Ror2*$^{TMLacZ/TMLacZ}$ mice showed absent pSMAD1/5/8 staining in distal mesenchyme (Fig. 1*E*). Together, these data suggest that a PFR is driving cartilage condensation during digit formation in the mouse, similar to the chick, and that Ror2^{W749X} interferes with PFR function, thus causing brachydactyly.

PFR Failure in *Ror2*$^{W749X/W749X}$ Mutants Causes Impaired Elongation of the Digit Condensation. To address the pathomechanism leading to loss of p2 in the *Ror2*$^{W749X/W749X}$ mouse, we monitored the appearance and differentiation of cartilaginous condensations in the autopod at embryonic day 12.5 (E12.5) to E14.5, the time when the phalanges are formed and become separated by joints. Whole-mount ISH for *Collagen type 2 alpha 1* (*Col2a1*) showed that the initial cartilage elements of the autopod at E12.5 were only slightly shorter in the mutant when compared with the WT (Fig. 2*A*). At E13.5 the metacarpal arising from the initial condensation showed a normal length, whereas the distal condensations that give rise to the growing phalanges were severely reduced in length (Fig. 2*A*). Longitudinal sections of the autopod immunolabeled with a SOX9 antibody (Fig. 2*B*) also showed almost normally sized condensations of the metacarpal at E12.5 and the proximal phalanx (p1) at E13.5. However, the distal-most condensations giving rise to the phalanges 2 and 3 (p2/3) showed severe shortening in mutant mice at E13.5. This led to a striking reduction in distal cartilage size at E14.5, a time at which the activity of the AER ceases and the distal-most condensation in the autopod starts to differentiate into a terminal phalanx (2). This indicates a defect in digit elongation after the establishment of the initial condensations in the autopod in *Ror2*$^{W749X/W749X}$ mice. Consistently, the phalangeal elongation defect is specific for the *Ror2*^{W749X} allele, because comparison of distal p2/3 length between WT, *Ror2*$^{-/-}$, and *Ror2*$^{W749X/W749X}$ mice at E13.5 confirmed that the p2/3 condensation is slightly shortened in the *Ror2*$^{-/-}$ mutant but is markedly reduced in the *Ror2*$^{W749X/W749X}$ mouse (Fig. S2).

Impaired Digit Elongation in *Ror2*$^{W749X/W749X}$ Mutants Is Caused by Defective Commitment of Mesenchymal Cells to the Cartilage Lineage. In the chick, the PFR controls digit elongation via cartilaginous commitment of mesenchymal progenitors (3, 4). To determine the rate of cell commitment into the growing cartilage condensation, we quantified the incorporation of mesenchymal cells into the distal condensations using BrdU pulse-chase labeling (6). Pregnant *Ror2*$^{+/W749X}$ mice were pulse-chase labeled with BrdU at E13.5 and analyzed at E14. Importantly, 1 h pulse labeling with BrdU does not result in a staining in the condensed cartilage but only in the surrounding mesenchyme (6). Coimmunostaining for BrdU and SOX9 ensured that only cartilage cells were counted. The results show a dramatic decrease in mesenchymal cell recruitment into the distal condensation (p2/3), which was reduced to less than 20% of WT values (Fig. 2*C*). One hour BrdU pulse labeling showed no differences in subridge mesenchyme proliferation rates (Fig. 2*C*). Compatible with a condensation defect, LacZ staining on *Ror2*$^{TMLacZ/+}$ mice, which are phenotypically normal (10), confirmed expression of ROR2 within cartilage condensations and in distal mesenchymal cells undergoing chondrogenesis in the autopod (Fig. S3). Micromass cultures derived from E12.5 hand plate mesenchymal cells stained with Alcian blue

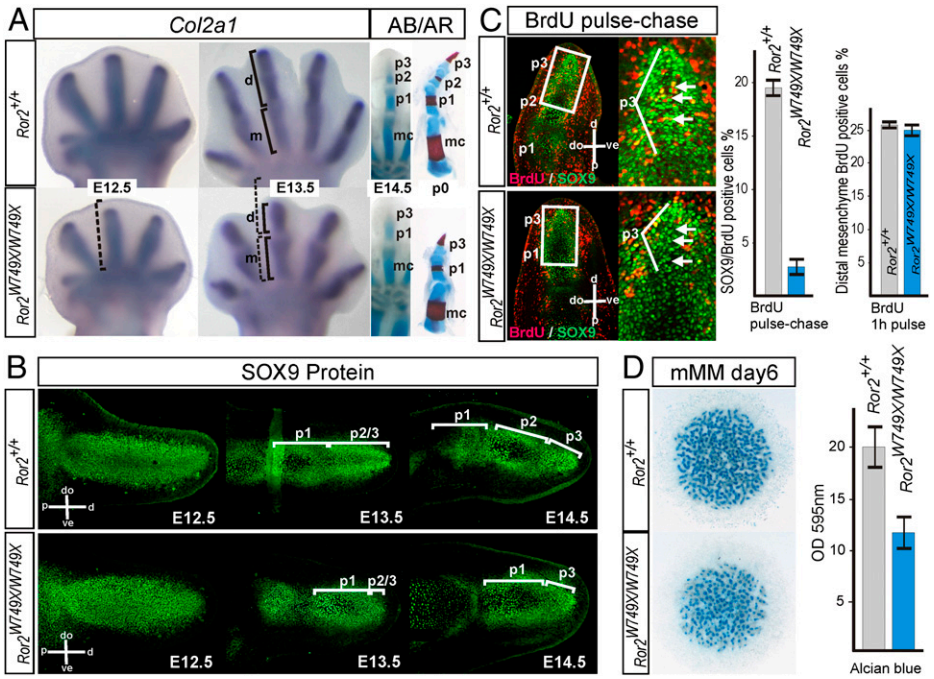

Fig. 2. Defective distal elongation after establishment of the initial condensation causes digit shortening in the *Ror2*$^{W749X/W749X}$ mutant via perturbed commitment of mesenchymal cells to cartilage. (*A*) Cartilage formation in the autopod between E12.5 and E14.5 visualized by whole-mount ISH for *Collagen type 2 alpha 1* (*Col2a1*) and by Alcian blue (AB) staining. At E12.5 the initial condensations in the autopod of the *Ror2*$^{W749X/W749X}$ mice are only slightly shortened (bracket shows length of WT condensation for comparison). At E13.5 the digit condensations (d) exhibit a marked shortening in the *Ror2*$^{W749X/W749X}$ mice, resulting in reduced distal phalangeal condensations at E14.5 visualized by Alcian blue (AB) staining. Alcian blue and Alizarin red (AR) staining of a p0 (newborn) digit 3 is shown for comparison; note missing middle phalanx (p2) and terminal phalanx (p3)-like appearance of the most distal element. (*B*) Anti-SOX9 antibody staining on longitudinal sections through a digit 3 demonstrating a decrease in cartilage formation distal to the first phalanx in the *Ror2*$^{W749X/W749X}$ mutant. Note that the *Ror2*$^{W749X/W749X}$ limb buds are wider than WT limb buds but have a normal length at E12.5. (*C*) BrdU pulse-chase experiment: 1 h pulse of BrdU at E13.5 was used to label mesenchymal cells and then, after blocking further incorporation of BrdU with excess thymidine, their fate was analyzed after 10 h. Sections were stained for BrdU (red) and SOX9 (green). Strong incorporation of mesenchymal cells into the SOX9-positive cartilage condensation was seen in the WT (*Ror2*$^{+/+}$), where numerous BrdU positive cells can be seen in the core of the cartilage condensation (arrows). In the *Ror2*$^{W749X/W749X}$ mutant, no BrdU-positive cells were observed in the core of the distal condensation. Quantification of SOX9/BrdU-positive cells in the distal condensation is shown to the right. Quantification of 1 h BrdU pulse labeling shows normal proliferation in distal mesenchyme. Error bars depict SEs deduced from at least three independent experiments. (*D*) Micromass cultures derived from E12.5 hand plates stained with Alcian blue for cartilage matrix, showing reduced chondrogenic potential of *Ror2*$^{W749X/W749X}$ mesenchyme. Colorimetric quantification of Alcian blue staining from at least three independent experiments is shown to the right. m, metacarpal; p1, p2, p3, condensations of phalanges 1, 2 and 3, respectively; p2/3, unseparated primordium of phalanges 2 and 3. Orientation of sections as indicated; dorsal (do), ventral (ve), proximal (p), and distal (d).

for cartilage nodules confirmed a reduced chondrogenic potential of the *Ror2*$^{W749X/W749X}$ mesenchyme compared with WT (Fig. 2*D*).

Altogether, these data indicate that a defect in chondrogenesis at a time crucial for the formation of the distal phalanges (between E13.5 and E14.5) is responsible for the digit shortening. Given that we have previously excluded a defect in the proliferation within the cartilage condensations by BrdU pulse labeling (9), the brachydactyly phenotype in the *Ror2*$^{W749X/W749X}$ mouse is not caused by a defect in the size of the initial condensation or its proliferative expansion but a failure of commitment of mesenchymal cells to the cartilage lineage.

Requirement of Mesenchymal IHH Signaling for the BMP/pSMAD1/5/8 Pathway in the PFR. BDB1 and BDA1 share similar digit features, and a mouse model (*Ihh*$^{E95K/E95K}$) for BDA1 carrying a human mutation (p.E95K) in *IHH* targeted to the mouse *Ihh* locus exhibits hypoplastic middle phalanges partially overlapping with the *Ror2*$^{W749X/W749X}$ mouse. Interestingly, the digit phenotype in the *Ihh*$^{E95K/E95K}$ mutant was caused by a similar, albeit weaker, impairment of chondrogenic cell commitment due to a disruption of the IHH pathway in the distal mesenchyme (6), indicating a common mechanism for both mutant phenotypes. Compared with WT littermates that showed normal pSMAD1/5/8 staining in the PFR and also in the cartilaginous condensations at E13.5 (Fig. 3*A*), in *Ihh*$^{E95K/E95K}$ mutant mice we observed a reduced pSMAD1/5/8 staining in the PFR and in the cartilage condensations (Fig. 3*B*). In accordance with the milder phenotype seen in the *Ihh*$^{E95K/E95K}$ mutants, pSMAD1/5/8 staining was reduced to a lesser degree than in the *Ror2*$^{W749X/W749X}$ mice.

To further substantiate the involvement of IHH signaling in the regulation of BMP signaling in the PFR, we used the *short digits* mouse mutant (*Dsh*/+) that also shows a BDA1 phenotype. The *Dsh*/+ phenotype is due to an up-regulated *Pthlh* expression from ectopic *Shh* expression, leading to a suppressed *Ihh* expression in distal phalanges (11), hence a mechanism comparable to the *Ihh*$^{E95K/E95K}$ mice (6). Immunolabeling for pSMAD1/5/8 also showed a reduced signal in the PFR of *Dsh*/+ mice (Fig. 3*C*). Together, these results indicate a critical involvement of the BMP/pSMAD1/5/8 signaling pathway in the pathogenesis of the

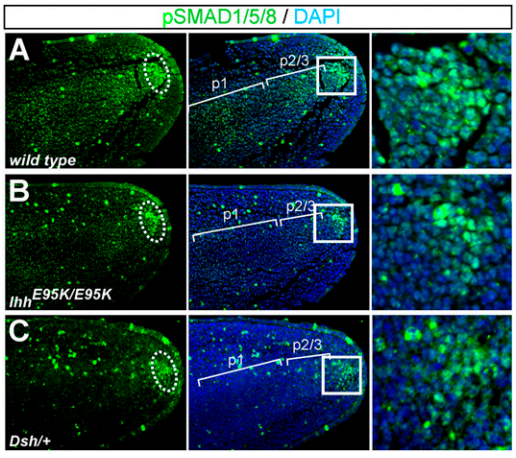

Fig. 3. BMP/pSMAD1/5/8 signaling in the PFR is decreased in *Ihh*$^{E95K/E95K}$ and *Dsh*/+ mouse models for BDA1. (*A*–*C*) Immunostaining for pSMAD1/5/8 (green) demonstrates down-regulation of distal BMP/SMAD1/5/8 signaling in the PFR of both mutants. Boxed regions are shown as magnifications. Note that pSMAD1/5/8 staining is also decreased within the condensations in *Ihh*$^{E95K/E95K}$ and *Dsh*/+ mutants compared with WT.

BDB1 and BDA1 phenotypes, indicating a potential common pathomechanism for BDB1 and BDA1, whereby ROR2 and IHH signaling might interact during digit elongation.

Genetic Interaction of *Ror2*$^{+/W749X}$ and *Ihh*$^{+/E95K}$ Mutations Indicate Cooperation of IHH and ROR2 Signaling. To further test this hypothesis, we crossed the *Ror2*$^{+/W749X}$ and *Ihh*$^{+/E95K}$ mice to test for genetic interaction. *Ror2*$^{+/W749X}$ mice show no digit phenotype, whereas *Ihh*$^{+/E95K}$ mice exhibit mild shortening of p2 in digits 2 and 5. *Ihh*$^{E95K/E95K}$ mice show a loss of p2 in digit 5 and severely reduced p2 in digits 2–4 (6). Compound *Ror2*$^{+/W749X}$ and *Ihh*$^{+/E95K}$ heterozygous mice showed severe reduction of p2 in digits 2 and 3, which was more prominent than the effect of the single *Ihh*^{E95K} allele, indicating a genetic interaction (Fig. 4 *A* and *B* and Fig. S4). Again, this effect was specific to the *Ror2*^{W749X} allele, because *Ror2*$^{+/-}$; *Ihh*$^{+/E95K}$ heterozygous mice showed no compound effect for the digit phenotype (Fig. 4*B*). When one *Ror2*^{W749X} allele was crossed to a homozygous *Ihh*$^{E95K/E95K}$ background, we observed a complete loss of the second phalanx in digits 2 and 3 (Fig. 4*C* and Fig. S4), phenocopying *Ror2*$^{W749X/W749X}$ mice and being more severe than in *Ihh*$^{E95K/E95K}$ mice. This suggests that both IHH and ROR2 act, at least in part, independently of each other in digit elongation. Loss or severe reduction of the terminal phalanges and nails is a hallmark of human BDB1 that is not recapitulated in the *Ror2*$^{W749X/W749X}$ mice, probably owing to the high regenerative potential of digit tips in mice. However, when crossing one *Ihh*^{E95K} allele on a *Ror2*$^{W749X/W749X}$ background, a severely hypoplastic terminal phalanx was observed (Fig. 4*D*), suggesting an involvement of the IHH pathway in the pathogenesis of BDB1 and a contribution of IHH signaling to the phenotype seen in *Ror2*$^{W749X/W749X}$ mutants.

Decreased IHH Signaling in the Distal Mesenchyme of *Ror2*$^{W749X/W749X}$ Mutants. To assess the involvement of IHH signaling in the BDB1 phenotype, we analyzed expression of *Ihh* and IHH downstream targets in *Ror2*$^{W749X/W749X}$ mice. Whole-mount ISH showed a decrease of *Ihh* expression in *Ror2*$^{W749X/W749X}$ mice compared with WT at stage E13.5 (Fig. 5*A*). Interestingly, distal *Ihh* expression was restored at E14.5, coinciding with the formation and differentiation of a distal phalanx (tip structure) (Fig. 5*A*). Analysis of IHH pathway targets *Gli1*, *Ptc1*, and *Runx2* in *Ror2*$^{W749X/W749X}$ mice at E13.5 showed a strong down-regulation of the IHH signaling pathway not only in the distal condensations but also in the undifferentiated distal mesenchyme (Fig. 5*B*), to a level comparable to that in *Ihh*$^{E95K/E95K}$ mice (6).

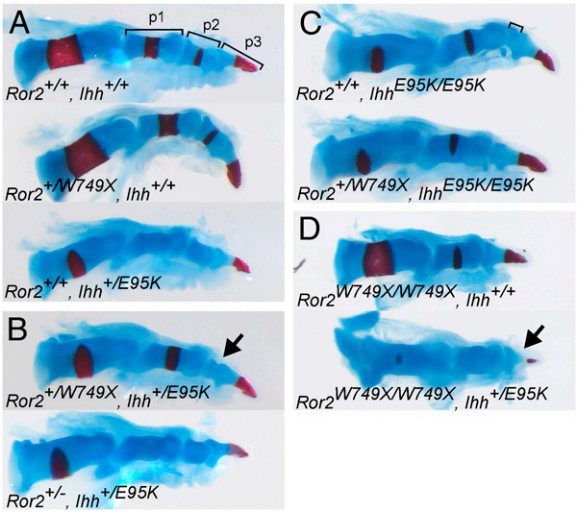

Fig. 4. Genetic interaction of *Ror2*^{W749X} (BDB1 mutation) and *Ihh*^{E95K} (BDA1 mutation). Skeletal preparations stained for cartilage (Alcian blue) and bone (Alizarin red) of digit 2 from newborn mice of the indicated allelic combinations are shown. (*A*) Single heterozygous *Ror2*$^{+/W749X}$ mutants have a WT appearance, whereas *Ihh*$^{+/E95K}$ mutants show a mild reduction in p2 length. (*B*) Compound Ror2$^{+/W749X}$; Ihh$^{+/E95K}$ mutants show severely reduced middle phalanx (arrow). The genetic interaction is specific for the *Ror2*^{W749X} allele, because a *Ror2* null allele does not show genetic interaction with *Ihh*^{E95K}. (*C*) The phenotype of the homozygous *Ihh*$^{E95K/E95K}$ (reduced p2 size) is enhanced by addition of one *Ror2*^{W749X} allele, where the middle phalanx is now missing. (*D*) Similarly, the addition of one *Ihh*^{E95K} allele on the *Ror2*$^{W749X/W749X}$ background also enhances severity of the phenotype leading to a hypoplastic distal phalanx (arrow).

Ectopic WNT/β-Catenin Signaling in Ror2$^{W749X/W749X}$ Mutants. Because the *Ror2*$^{W749X/W749X}$ mutant displays a more pronounced digit phenotype than the *Ihh*$^{E95K/E95K}$ mutant, and human BDB1 exhibits a more severe phenotype than BDA1, a disruption of IHH signaling in the *Ror2*$^{W749X/W749X}$ mutant cannot be solely responsible for the phenotype. ROR2 is known as an alternative WNT coreceptor involved in the negative regulation of canonical WNT/β-catenin signaling (8). ISH analysis for WNT/β-catenin signaling targets *Itf-2* and *Nmyc* indicated an ectopic activation of canonical WNT signaling in the distal mesenchyme of *Ror2*$^{W749X/W749X}$ mice (Fig. S5*A*). Next, we performed immunostaining for dephosphorylated (activated) β-catenin. Sections were costained for SOX9 to ensure that correct planes were compared. Equally strong signals were observed in the muscles of WT and *Ror2*$^{W749X/W749X}$ mice; however, in the distal limb mesenchyme and also the distal SOX9-positive cell population, the β-catenin signal was significantly stronger in *Ror2*$^{W749X/W749X}$ mice than in WT mice (Fig. S5*B*). To definitively demonstrate ectopic WNT/β-catenin signaling in the distal limb, we crossed *Ror2*$^{+/W749X}$ mice with the *Axin2*^{LacZ} reporter mice (12). LacZ staining of cryosections at E13.5 showed a strong WNT/β-catenin signal in the ectoderm and in the superficial mesenchyme, as reported previously for the early limb bud (13). However, the distal superficial mesenchyme (subridge mesenchyme) and the cells undergoing chondrogenesis showed absent or low WNT/β-catenin signaling in WT embryos (Fig. 5*C*, arrows), although these cells are in the range of WNTs emanating from the ectoderm, indicating that β-catenin signaling is suppressed in this area. In *Ror2*$^{W749X/W749X}$ mice, the distal mesenchyme and the distal condensation showed intense LacZ staining, indicating ectopic activation of the WNT/β-catenin pathway (Fig. 5*C*, arrows). This finding was also corroborated by whole-mount LacZ staining (Fig. S5*C*). Finally, to quantify the increase of canonical WNT signaling, we performed micromass cultures of mesenchymal cells from hand plates of E12.5 *Ror2*$^{+/+}$/*Axin2*^{LacZ} and *Ror2*$^{W749X/W749X}$/*Axin2*^{LacZ} embryos. Histomorphometric analysis of LacZ staining as an indicator of WNT/β-catenin signaling showed an increase in cultures derived from *Ror2*$^{W749X/W749X}$ mice by an average of 2.5-fold compared with WT levels (Fig. 5*D*).

Discussion

We have shown here that a defect in the PFR underlies digit shortening in mouse models for human BDA1 and BDB1 via a down-regulation of chondrogenic cell commitment, demonstrating that in mammals BMP/SMAD1/5/8 signaling in the PFR is instrumental in driving digit elongation and thus determination of phalanx numbers. Our results indicate that both IHH and ROR2 are acting independently upstream of BMP/SMAD1/5/8 signaling in the mammalian PFR, as summarized in Fig. 5*E*.

IHH signaling is essential for normal development of the phalanges in mouse and human (6, 14). IHH emanating from the cartilage condensation signals to the distal undifferentiated mesenchyme, regulating chondrogenic commitment of mesenchymal cells via an unknown mechanism (6). We propose that IHH influences distal chondrogenesis via BMP signaling. Hedgehogs regulate *Bmps* in different organisms from *Drosophila* to human, and in various developmental contexts including the cartilage growth plate and the limb bud (15, 16). Thus, the positive effect of

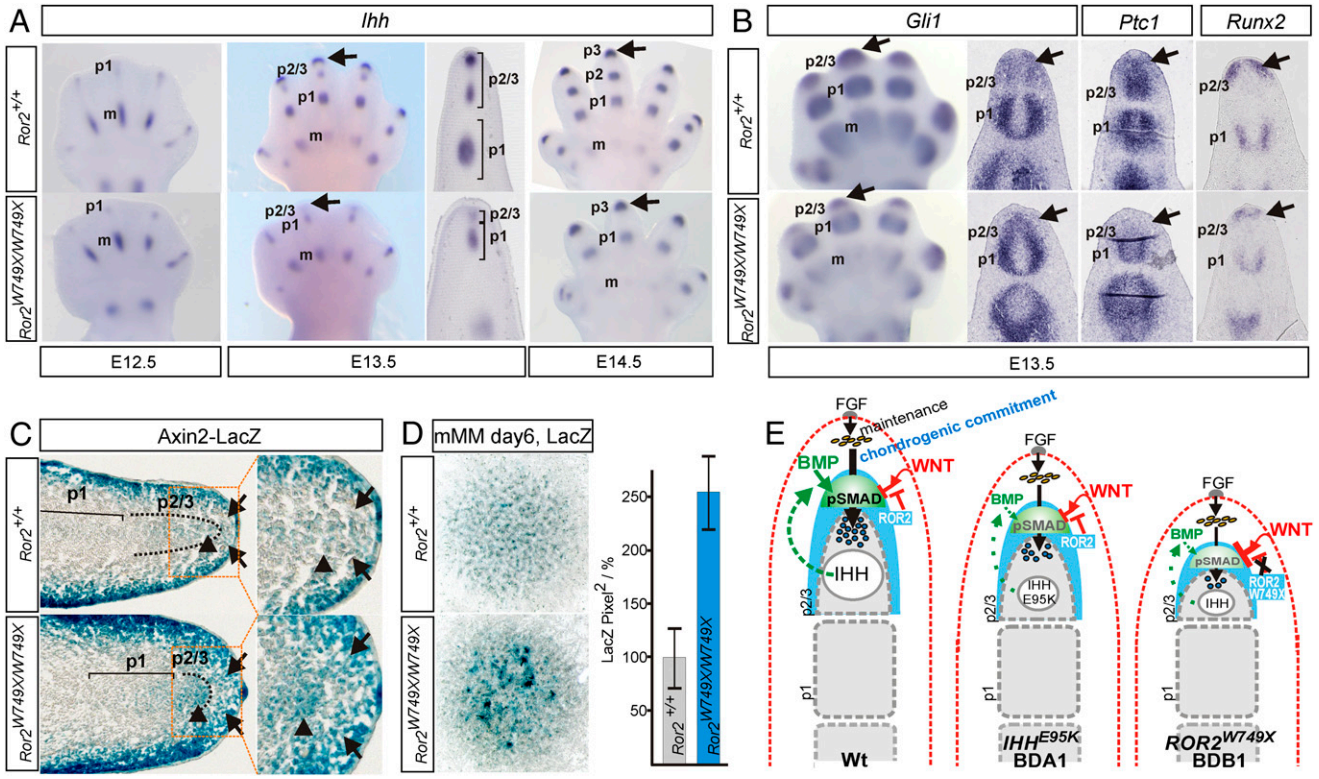

Fig. 5. Dysregulation of IHH and canonical WNT pathways in *Ror2*$^{W749X/W749X}$ mutants. (*A*) Whole-mount ISH showing a down-regulated distal expression of *Ihh* in *Ror2*$^{W749X/W749X}$ mutant hand plates at E13.5 (arrows) that recovered concomitant with the differentiation of the digit tip at E14.5 (arrows). (*B*) Down-regulation of the IHH pathway in distal mesenchyme shown by whole-mount and section ISH for the IHH targets *Gli1*, *Ptc1*, and *Runx2*. (*C*) *Ror2*^{W749X} line crossed to the canonical WNT reporter line *Axin2*^{LacZ}, demonstrating ectopic activation of the canonical WNT pathway in *Ror2*$^{W749X/W749X}$ mice. LacZ staining on cryosections shows elevated/ectopic signal in the mutant in distal mesenchyme (arrows) and also in the distal-most condensation (arrowheads). Boxed areas are shown as magnifications. (*D*) Micromass cultures of E12.5 hand plates derived from *Ror2*$^{W749X/W749X}$/*Axin2*^{LacZ} embryos showing increased LacZ activity in cultures derived from mutant embryos. *Right:* Histomorphometrical quantification; error bars represent SEs from three independent experiments. (*E*) Schematic representation of pathway network regulating digit outgrowth in WT and its perturbation in the *Ihh*$^{E95K/E95K}$ and the *Ror2*$^{W749X/W749X}$ mutants leading to impaired distal elongation of the digit condensations in the BDA1 and BDB1 phenotypes. AER–FGF signaling maintains undifferentiated mesenchymal cells (yellow). BMP/pSMAD1/5/8 signaling in the PFR (green) mediates distal outgrowth of the phalangeal condensation by controlling commitment of mesenchymal cells (arrow) to the condensation. IHH promotes distal outgrowth by enhancing chondrogenic cell commitment, potentially via induction of mesenchymal BMPs. Canonical WNT factors emanating from the ectoderm (red) induce β-catenin signaling in the mesenchyme, which inhibits BMP/pSMAD1/5/8 signaling in the PFR, thus limiting distal growth. The β-catenin signaling in the mesenchyme is negatively regulated by ROR2 (strong expression domain of ROR2 in condensing distal mesenchyme is highlighted in blue). In BDA1, the IHH^{E95K} protein interferes with normal IHH signaling in distal mesenchyme, subsequently leading to a down-regulation of the BMP pathway in the PFR. In BDB1, the expression of a truncated ROR2 molecule leads to an up-regulation of WNT/β-catenin signaling in the mesenchyme concomitant with a down-regulation of *Ihh* expression and pathway activation, both converging on a drastic down-regulation of BMP/pSMAD1/5/8 signaling in the PFR. m, metacarpal; p1, condensation of phalanx 1; p2/3, unseparated primordium of phalanges 2 and 3.

IHH on distal chondrogenesis required for digit growth might be mediated, at least in part, by induction of prochondrogenic BMPs. In support of this hypothesis, mice with inactivated alleles of *Ihh* (17) showed a strong decrease of *Bmp4* expression in the distal mesenchyme (Fig. S6).

Concomitant with the breakdown of BMP/pSMAD1/5/8 signaling in *Ror2*$^{W749X/W749X}$ mice, we observed an increase in canonical WNT/β-catenin signaling in the distal limb mesenchyme. WNT/β-catenin signaling can inhibit cartilage differentiation in vitro and in vivo (13, 18, 19) and acts antagonistic to BMP/SMAD signaling in cartilage formation (20, 21). Consistently, our results also point toward a negative role for WNT/β-catenin signaling in the cascade of events leading to the activation of BMP/SMAD signaling during digit elongation, by inhibiting either the formation or the maintenance of the PFR. The hypothesis that up-regulation of canonical WNT signaling might cause a brachydactyly phenotype is supported by mice devoid of the WNT antagonists SFRP1 and SFRP2, which develop a digit phenotype reminiscent of the *Ror2*$^{W749X/W749X}$ mice (22).

ROR2 was shown to be an alternative WNT receptor, mainly for WNT5A (8, 23), and WNT5A can inhibit the canonical WNT pathway via ROR2 (8). WNT5A has a vital role in promoting digit formation, because *Wnt5a*$^{-/-}$ mice lack proximal and middle phalanges (24). It has also been shown that WNT5A acts as a negative regulator of WNT/β-catenin signaling in distal limb mesenchyme in vivo (25). In addition to signaling via ROR2, it is likely that WNT5A has further functions because *Wnt5a*$^{-/-}$ mice have a more severe digit phenotype than *Ror2*$^{-/-}$ mice (23). WNT5A is known to signal via Frizzled receptors to noncanonical pathways including the WNT/calcium pathway (26), which can also inhibit the β-catenin pathway (27). Thus it is conceivable that the truncated ROR2 protein might act as a scavenger for WNT5A, thus inhibiting WNT5A signaling pathways. Interestingly such a scavenger-like function has been proposed for the *Caenorhabditis elegans* ROR ortholog CAM-1, which is lacking the C-terminal domain equivalent to mouse/human ROR2 p.W749X (28).

Limb outgrowth and digit elongation also requires intact AER–FGF signaling, which drives subridge mesenchyme proliferation and prevents premature initiation of the terminal phalanx (2). No

premature regression of the AER was observed in $Ror2^{W749X/W749X}$ or $Ihh^{E95K/E95K}$ mice (6, 9). At E14.5, the remaining distal cartilage is undergoing the program for tip formation in $Ror2^{W749X/W749X}$ mice, at the appropriate time as in WT mice, concordant with a reactivation of *Ihh* expression. Furthermore, precocious AER ablation is accompanied by apoptosis in the underlying mesoderm (29). We also tested for apoptosis rates by immunostaining for active caspase 3 but found no differences between WT and mutant mice in mesenchyme or in condensations (Fig. S7). This argues against an involvement of AER–FGF signaling in the phenotypes of the $Ror2^{W749X/W749X}$ and $Ihh^{E95K/E95K}$ mutants and hence in the pathogenesis of human BDB1 or BDA1.

In the context of the disease mechanism for BDA1 and BDB1 (Fig. 5*E*), in BDA1 IHH^{E95K} exhibits a negative effect on distal mesenchymal IHH signaling (6), thus resulting in lowered BMP/pSMAD1/5/8 signaling in the PFR. However, chondrogenesis is robust enough to result in a condensation that exceeds the minimal size for the formation of an additional joint, resulting in a shortened p2. In BDB1, *Ihh* expression and pathway activation is diminished by a yet-unknown mechanism. In addition to that, $ROR2^{W749X}$ interferes with the inhibition of canonical WNT/β-catenin signaling in the distal mesenchyme and the nascent condensation. This altogether results in a drastic reduction of BMP/pSMAD1/5/8 signaling, strongly impairing chondrogenesis and digit elongation. This results in a distal condensation (p2/3) that is too small for the formation of an additional joint. At E14.5 the remaining cartilage undergoes differentiation to a terminal phalanx, and hence the middle phalanx is lost.

In summary, this work demonstrates that a signaling center analogous to the chicken PFR/digit crescent exists in mammals and uncovers genetic mechanisms controlling digit development, with both IHH and ROR2 acting cooperatively to fine-tune BMP signaling in the PFR. In consequence this proposes a pathomechanism for human brachydactylies A1 and B1 via disrupted BMP/SMAD1/5/8 signaling, the pathway affected in brachydactylies A2, B2, and C. This suggests that the distinct yet overlapping phenotypes observed in the brachydactyly disease family can be explained by a unifying molecular network converging on BMP signaling.

Materials and Methods

In Situ Hybridizations. ISHs on whole-mount embryos as well as on paraffin sections were performed as previously described (30).

Immunohistochemistry. Immunohistochemistry was done on paraffin sections. Antigen retrieval was performed using citrate buffer or high-pH buffer (Dako). After permeabilization with 0.2% Triton X-100 for 15 min and blocking with 5% normal goat serum, primary antibody incubation was performed at 4 °C overnight and detection with fluorescence-conjugated secondary antibody (Molecular Probes, Invitrogen) at room temperature for 1 h. For phospho-SMAD staining, additional biotinyl tyramid signal amplification was performed according to the manufacturer's protocol (Perkin-Elmer).

BrdU Pulse-Chase Labeling. Mice were injected i.p. with 200 μg BrdU per gram of body weight. After 1 h, incorporation into DNA was blocked by injection of a 30-fold excess of thymidine, and mice were killed after a further 10 h. Statistical analysis was performed by counting BrdU/SOX9 dual-positive cells relative to SOX9-positive cells on four sections for three of each WT and mutant specimen.

Mouse micromass cultures were prepared from E12.5 hand plates according to standard procedures. Cultures were stained with Alcian blue and quantified photometrically.

All animal experiments were carried out in compliance with legal requirements of the European Union.

Detailed materials and methods are available in *SI Materials and Methods*.

ACKNOWLEDGMENTS. We thank Kathrin Seidel and Norbert Brieske for their expert technical assistance and the animal facility of the Max Planck Institute for Molecular Genetics, especially Janine Wetzel, for mouse work assistance. This project was funded by Deutsche Forschungsgemeinschaft Grant SFB 577 (to S.S. and S.M.) and Research Grants Council of Hong Kong Grant HKU760608M (to D.C.).

1. Zeller R, López-Ríos J, Zuniga A (2009) Vertebrate limb bud development: Moving towards integrative analysis of organogenesis. *Nat Rev Genet* 10:845–858.
2. Casanova JC, Sanz-Ezquerro JJ (2007) Digit morphogenesis: Is the tip different? *Dev Growth Differ* 49:479–491.
3. Suzuki T, Hasso SM, Fallon JF (2008) Unique SMAD1/5/8 activity at the phalanx-forming region determines digit identity. *Proc Natl Acad Sci USA* 105:4185–4190.
4. Montero JA, Lorda-Diez CI, Gañan Y, Macias D, Hurle JM (2008) Activin/TGFbeta and BMP crosstalk determines digit chondrogenesis. *Dev Biol* 321:343–356.
5. Mundlos S (2009) The brachydactylies: A molecular disease family. *Clin Genet* 76:123–136.
6. Gao B, et al. (2009) A mutation in Ihh that causes digit abnormalities alters its signalling capacity and range. *Nature* 458:1196–1200.
7. Green JL, Kuntz SG, Sternberg PW (2008) Ror receptor tyrosine kinases: Orphans no more. *Trends Cell Biol* 18:536–544.
8. Mikels AJ, Nusse R (2006) Purified Wnt5a protein activates or inhibits beta-catenin-TCF signaling depending on receptor context. *PLoS Biol* 4:e115.
9. Raz R, et al. (2008) The mutation ROR2W749X, linked to human BDB, is a recessive mutation in the mouse, causing brachydactyly, mediating patterning of joints and modeling recessive Robinow syndrome. *Development* 135:1713–1723.
10. DeChiara TM, et al. (2000) Ror2, encoding a receptor-like tyrosine kinase, is required for cartilage and growth plate development. *Nat Genet* 24:271–274.
11. Niedermaier M, et al. (2005) An inversion involving the mouse Shh locus results in brachydactyly through dysregulation of Shh expression. *J Clin Invest* 115:900–909.
12. Lustig B, et al. (2002) Negative feedback loop of Wnt signaling through upregulation of conductin/axin2 in colorectal and liver tumors. *Mol Cell Biol* 22:1184–1193.
13. ten Berge D, Brugmann SA, Helms JA, Nusse R (2008) Wnt and FGF signals interact to coordinate growth with cell fate specification during limb development. *Development* 135:3247–3257.
14. Gao B, et al. (2001) Mutations in IHH, encoding Indian hedgehog, cause brachydactyly type A-1. *Nat Genet* 28:386–388.
15. Drossopoulou G, et al. (2000) A model for anteroposterior patterning of the vertebrate limb based on sequential long- and short-range Shh signalling and Bmp signalling. *Development* 127:1337–1348.
16. Minina E, Kreschel C, Naski MC, Ornitz DM, Vortkamp A (2002) Interaction of FGF, Ihh/Pthlh, and BMP signaling integrates chondrocyte proliferation and hypertrophic differentiation. *Dev Cell* 3:439–449.
17. St-Jacques B, Hammerschmidt M, McMahon AP (1999) Indian hedgehog signaling regulates proliferation and differentiation of chondrocytes and is essential for bone formation. *Genes Dev* 13:2072–2086.
18. Rudnicki JA, Brown AM (1997) Inhibition of chondrogenesis by Wnt gene expression in vivo and in vitro. *Dev Biol* 185:104–118.
19. Hill TP, Später D, Taketo MM, Birchmeier W, Hartmann C (2005) Canonical Wnt/beta-catenin signaling prevents osteoblasts from differentiating into chondrocytes. *Dev Cell* 8:727–738.
20. Akiyama H, et al. (2004) Interactions between Sox9 and beta-catenin control chondrocyte differentiation. *Genes Dev* 18:1072–1087.
21. Fischer L, Boland G, Tuan RS (2002) Wnt signaling during BMP-2 stimulation of mesenchymal chondrogenesis. *J Cell Biochem* 84:816–831.
22. Satoh W, Gotoh T, Tsunematsu Y, Aizawa S, Shimono A (2006) Sfrp1 and Sfrp2 regulate anteroposterior axis elongation and somite segmentation during mouse embryogenesis. *Development* 133:989–999.
23. Oishi I, et al. (2003) The receptor tyrosine kinase Ror2 is involved in non-canonical Wnt5a/JNK signalling pathway. *Genes Cells* 8:645–654.
24. Yamaguchi TP, Bradley A, McMahon AP, Jones S (1999) A Wnt5a pathway underlies outgrowth of multiple structures in the vertebrate embryo. *Development* 126:1211–1223.
25. Topol L, et al. (2003) Wnt-5a inhibits the canonical Wnt pathway by promoting GSK-3-independent beta-catenin degradation. *J Cell Biol* 162:899–908.
26. Slusarski DC, Yang-Snyder J, Busa WB, Moon RT (1997) Modulation of embryonic intracellular Ca2+ signaling by Wnt-5A. *Dev Biol* 182:114–120.
27. Ishitani T, et al. (2003) The TAK1-NLK mitogen-activated protein kinase cascade functions in the Wnt-5a/Ca(2+) pathway to antagonize Wnt/beta-catenin signaling. *Mol Cell Biol* 23:131–139.
28. Green JL, Inoue T, Sternberg PW (2007) The *C. elegans* ROR receptor tyrosine kinase, CAM-1, non-autonomously inhibits the Wnt pathway. *Development* 134:4053–4062.
29. Rowe DA, Cairns JM, Fallon JF (1982) Spatial and temporal patterns of cell death in limb bud mesoderm after apical ectodermal ridge removal. *Dev Biol* 93:83–91.
30. Stricker S, et al. (2006) Cloning and expression pattern of chicken Ror2 and functional characterization of truncating mutations in Brachydactyly type B and Robinow syndrome. *Dev Dyn* 235:3456–3465.